Environmental Science Nano

PAPER

View Article Online
View Journal | View Issue

Cite this: *Environ. Sci.: Nano*, 2018, 5, 520

Foliar surface free energy affects platinum nanoparticle adhesion, uptake, and translocation from leaves to roots in arugula and escarole†

Eva Kranjc, *[ab] Darja Mazej,[c] Marjana Regvar, [d] Damjana Drobne[d] and Maja Remškar[b]

Pt nanoparticles (NPs) are directly emitted into air from human activities, contributing to the pollutant load of plants and posing risks to food safety. Foliar surface characteristics affect particle interception and retention from air; however the influence of foliar surface free energy (SFE), a quantitative measure of polar and dispersive surface forces which determine hydrophobicity/hydrophilicity, has not been investigated. Here, soil-grown plantlet leaves of arugula (low SFE) and escarole (high SFE) were exposed to Pt NPs (5–500 mg Pt NPs per L) for 5 days. Pt NP internalization and translocation, aggregation/agglomeration on leaf surfaces, and SFE changes were analyzed. Plantlets were also root-exposed to Pt NPs (one exposure to 20 mL of 50 mg L^{-1} dispersion) to provide a comparison between leaf-to-root and root-to-leaf translocation. Among foliar-exposed plants, inductively coupled plasma-mass spectrometry data showed that relative to escarole, arugula contained higher Pt concentrations in leaves (33, 31, and 14 times higher for 5, 50, and 500 mg L^{-1} exposures, respectively) and lower Pt concentrations in roots (6, 4, and 3 times lower for 5, 50, and 500 mg L^{-1} exposures, respectively). For both plants, the proportion of Pt translocated from roots to leaves (99% and 28% for arugula and escarole, respectively) was higher than that from leaves to roots (<1% for both plants). Scanning electron micrographs of foliar-exposed leaves (500 mg Pt NPs per L) showed a much higher degree of Pt NP aggregation/agglomeration on arugula relative to escarole, in addition to stomata closure from likely shading effects on arugula. Analysis of foliar SFE results based on acid–base theory did not indicate any relationship between Pt NP exposure and changes to SFE. We conclude that plants with low SFE are significantly more likely to adhere and retain NPs than plants with high SFE, providing implications for the application of nanopesticides, where NP adsorption and retention are of interest, and for food safety, where the presence of NPs should be minimized.

Received 22nd September 2017,
Accepted 17th December 2017

DOI: 10.1039/c7en00887b

rsc.li/es-nano

Environmental significance

Metallic pollutants, including Pt, are disproportionately emitted into air as nanoparticles (NPs), whose retention and uptake by plant leaves is affected by their foliar characteristics, such as wrinkling, waxiness, and the presence of trichomes. In this study, the influence of foliar surface free energy (SFE) on Pt NP retention and translocation was investigated using arugula (low SFE) and escarole (high SFE) plants. Our results show that low foliar SFE is significantly correlated with increased Pt NP retention and decreased internalization and translocation to roots due to stomata closure from likely shading effects. These results indicate that foliar SFE should be included as a relevant factor where environmental and food chain transfer and the development and use of agricultural nanomaterials are concerned.

[a] *Jožef Stefan International Postgraduate School, Jamova cesta 39, 1000 Ljubljana, Slovenia. E-mail: eva.kranjc@ijs.si, e.kranjc13@gmail.com; Tel: +386 31 589 327*
[b] *Department of Condensed Matter Physics, Jožef Stefan Institute, Jamova cesta 39, 1000 Ljubljana, Slovenia. E-mail: maja.remskar@ijs.si*
[c] *Department of Environmental Sciences, Jožef Stefan Institute, Jamova cesta 39, 1000 Ljubljana, Slovenia. E-mail: darja.mazej@ijs.si*
[d] *Department of Biology, Biotechnical Faculty, University of Ljubljana, Večna pot 111, 1000 Ljubljana, Slovenia. E-mail: marjana.regvar@bf.uni-lj.si, damjana.drobne@bf.uni-lj.si*

† Electronic supplementary information (ESI) available: Additional information about SFE methods used in this work, including eqn (S1)–(S4), Fig. S1–S7 and Tables S1–S10. See DOI: 10.1039/c7en00887b

1. Introduction

Atmospheric deposition of metallic nanoparticles (NPs) is a major, but understudied, contributor to the pollutant load of plants, posing risks to food safety, with the potential for food chain transfer and impacts on human health and ecosystem quality.[1,2] Anthropogenic metallic particle emissions are disproportionately concentrated in the finest particle size fractions,[3] which can also be quickly transported over great distances through the atmosphere.[4] Platinum NPs are a

component of this pollution due to their widespread use in automobile catalytic converters.[5] Other characteristics, such as low environmental background abundance in unpolluted environments (2.7 ppb)[6] and resistance to dissolution,[7] make it an ideal test NP materials when bioaccumulation, adsorption, organism translocation, or food chain transfer are studied.

Atmospheric NP deposits may adsorb onto and be taken up by plant foliar surfaces mostly through the cuticle and stomata,[8,9] exceeding pollutant uptake by roots from water and soil.[4] Schreck *et al.*[10,11] demonstrated that atmospheric deposition at industrial locations contributes more to plant foliar Pb concentrations than soil pollution. Al Jassir *et al.*[12] traced elevated concentrations of Pb, Cd, Cu, and Zn in roadside market vegetables in the city of Riyadh, Saudi Arabia to atmospheric deposition of automobile and industrial exhausts. Hu *et al.*[13] reported a substantial airborne contribution to the Pb concentration in leaves of *Aster subulatus* plants in Nanjing, China.

Although there have been studies that examine the uptake and translocation of NPs from roots to leaves,[14–22] only a few have investigated NP uptake and translocation from leaves to roots,[23–27] which may carry important implications for the effect of atmospheric deposition on pollutant concentrations of above-ground plant segments as well as on the safety of nanopesticide application. In the studies by Hong *et al.*,[24,25] elevated concentrations of Ce (40–320 mg CeO_2 NPs per L dispersions and 0.98 and 2.94 CeO_2 NPs per m^3 aerosol) and Cu (50 mg CuO NPs per L) were detected in the seedling roots of cucumber plants after foliar exposure. For equal applications of 100 mg L^{-1} solution, Wang *et al.*[23] quantified fractions of internalized and translocated NPs in the roots of leaf-exposed watermelon which were measured to be 1.23% (TiO_2 NPs), 5.74% (ZnO NPs), and 8.13% (MgO NPs). Although dissolution was not strictly monitored, CeO_2 and TiO_2 NPs are considered to be non-dissolvable. In plants, a very large surface area is available for atmospheric deposition and even if NP dissolution is low, the dissolved ions are able to cross the cuticle and cell wall where size exclusion limits (3.6–7.1 nm) do not present a physical barrier.[28]

In addition, plant leaf surface characteristics, such as wrinkling, waxiness, and the presence of trichomes, may significantly affect particle interception and retention from air.[10,29] Although leaf wettability, *i.e.* surface free energy (SFE), also plays a role in these processes,[11,29–31] there have been no prior attempts to characterize and assess its role in the context of foliar NP exposure. In the present work, we selected two plant species to study the effect of SFE on NP adhesion and uptake: arugula (*Eruca sativa* Mill.) and escarole (*Cichorium endivia* L.). Arugula has a considerably lower SFE than escarole, which means that there is less available surface energy to increase the surfaces of applied liquid droplets, resulting in a lower contact area between the droplet and leaf surface. Since contact between the foliar surface and liquid is necessary for internalization to occur, we hypothesized that there would be less uptake and translocation of NPs in arugula.[32] The leaves of the two species also differ in hairiness, with escarole containing trichomes and arugula containing none.

In this paper, scanning electron microscopy coupled to energy dispersive X-ray spectroscopy (SEM-EDX), three-liquid (*i.e.* ultrapure water, diiodomethane, and glycerol) acid–base theory,[33] and inductively coupled plasma-mass spectrometry (ICP-MS) were used to investigate and compare arugula and escarole responses to Pt NPs in terms of (a) foliar surface adsorption patterns, (b) foliar SFE, and (c) uptake and translocation of Pt NPs from exposed to unexposed plant segments, *i.e.* from leaves to roots and from roots to leaves. We discuss the implications of our findings for food safety and agricultural nanotechnologies.

2. Materials and methods

2.1 Pt NP characterization

Pt nanopowder (<50 nm) was purchased from Sigma-Aldrich. Its morphology and chemical composition were analyzed using SEM (JEOL JSM-7600F, Japan) coupled to EDX (INCA Wave 500, Oxford Instruments Analytical, Ltd., UK) and transmission electron microscopy (TEM; JEOL JEM-2010F, Japan). The average particle size and size distribution were obtained from a random sample of 300 particles from TEM images using ImageJ v. 1.50i software. The specific surface area was determined with the Brunauer–Emmett–Teller (BET) method using single point nitrogen adsorption with a FlowSorb II 2300 instrument (Micromeritics, USA). A 50 mg Pt NPs per L dispersion in ultrapure water was analyzed with dynamic light scattering (DLS) for the hydrodynamic size and zeta potential using a ZetaPALS instrument (Brookhaven Instruments Corporation, USA) using a red laser (λ = 658 nm) for illumination with a scattering angle of 90°.

2.2 Examination of Pt NP dissolution

Two methods were used to examine Pt NP dissolution in ultrapure water at the experimental concentrations (5, 50, and 500 mg Pt NPs per L): (i) ultrafiltration for 30 min at 1880 × *g* and 20 °C using Amicon Ultra-4 centrifugal filter units composed of regenerated cellulose (nominal molecular weight limit [NMWL] of 3 kDa), and (ii) ultracentrifugation for 30 min at 100 000 × *g* and 20 °C (Beckman Coulter L8-70 M class H preparative ultracentrifuge; fixed-angle 70 Ti rotor; 15 mL Beckman Coulter Quick-Seal Polyallomer Centrifuge Tubes, USA). The supernatant from both methods was acidified to 5% HNO_3 (Suprapur 65% HNO_3, Merck, Germany), however samples from ultracentrifugation were carefully removed with a pipette and filtered (0.45 μm, hydrophilic PVDF, Millipore Millex-HV, Germany) before this step. In addition, samples of 5, 50, and 500 mg Pt NPs per L dispersions were dissolved in a 1 : 1 ratio of dispersion to *aqua regia* (25%: Suprapur 65% HNO_3, Merck, Germany; 75%: *puriss. p.a.* 37% HCl, Merck, Germany) to assess the actual amount of Pt in the experimental dispersions. These samples were diluted to 5% HNO_3 (Suprapur 65% HNO_3, Merck, Germany) prior to analysis.

To examine the possibility that Pt NP dissolution was affected by application onto the foliar surfaces, arugula and escarole leaf samples exposed to the 500 mg Pt NPs per L dispersion (as described in section 2.4) were submerged in ultrapure water (final nominal concentration of 5 mg Pt NPs per L) and homogenized using a T10 basic ULTRA-TURRAX homogenizer (IKA®-Werke GmbH & Co. KG, Germany), as shown in Fig. S1.† The blended mixture was then treated by ultrafiltration and ultracentrifugation in the same manner as the bare dispersions. All samples were prepared in triplicate with at least one blank and analyzed for Pt content using ICP-MS (7500 series, Agilent Technologies, Inc., USA) as described in section 2.7.

2.3 Leaf surface characterization

Arugula has relatively hydrophobic leaves,[34] whereas escarole forms a head of relatively hydrophilic leaves. Hydrophobicity/hydrophilicity (*i.e.* wettability) is typically assessed by the contact angle formed by a droplet of water on the leaf surface, with lower contact angles (<90°; Fig. 1B) indicating a hydrophobic surface, and higher contact angles (>90°; Fig. 1C) indicating a hydrophilic surface.[33,35] The leaves of both may range from glabrous to mildly hairy. Unexposed and 500 mg Pt NPs per L foliar exposed lyophilized arugula and escarole leaf samples were mounted on a SEM holder with double-sided C tape and coated with ~10 nm Au using an SCD 005 cool sputter coater (BAL-TEC GmbH, Switzerland). The samples were then analyzed with SEM using an accelerating voltage of 15 kV under ultra-high vacuum conditions (9.6×10^{-5} Pa) operating in secondary electron mode. No fewer than 10 images (×250 magnification) of the abaxial and adaxial foliar surfaces were analyzed for stomatal density, proportion of open stomata, and morphological characteristics.

2.4 Plant cultivation and Pt NP exposure setup

Arugula and escarole were grown according to a modified version of OECD test no. 208 (terrestrial plant test: seedling emergence and seedling growth test) using plastic pots (diameter: 11 cm; height: 10 cm) filled with biological 100% finely milled peat (pH: 6.5; Bio Plantella START special soil for sowing and potting, Unichem LLC, Armenia). Ten seeds were placed into each pot, followed by the removal of 9 seedlings upon germination. Three replicates containing 5 plants each were cultivated for every exposure (15 plants in total). The soil pH was evaluated before planting and after the experimental period for control and Pt NP exposed plants using ISO 10390: soil quality – determination of pH. All plants were raised in growth chambers (day/night period: 16 h/8 h; temperature: 21 °C/17 °C; humidity: 45%/65%) with a photosynthetic photon flux density of 110 μmol m^{-2} s^{-1}. Plants were watered with tap water using a self-watering device to ensure constant and even hydration. An image of the plant cultivation setup is shown in Fig. S2A.†

After reaching a 4-leaf (arugula) or 5-leaf (escarole) growth stage, either the leaves or roots of the plants were exposed. Plants in the foliar exposure group were administered with Pt NPs dispersed in ultrapure water at concentrations of 5, 50, or 500 mg L^{-1} using a probe sonication procedure developed in accordance with the recommendations by Taurozzi *et al.*[36] Exposure was completed over a 5 day period during which abaxial and adaxial foliar surfaces were covered daily with 2 μL droplets applied with a pipette per 0.5 cm^2 leaf surface (Fig. S2B and C†).[37] On the day of each exposure during the 5 day exposure period, 10 mL of a 500 mg Pt NPs per L dispersion were prepared by pulse sonication (10 s pulse, 5 s rest) in a 2.5 cm diameter glass vial on ice for 3 min at 8.58 W. Soil surfaces were covered with Parafilm® to prevent unintended deposition onto soil. In the root exposure group, one application consisting of 20 mL of 50 mg Pt NPs per L dispersion was evenly applied to the soil surface. Following the week of exposure, plants were grown to maturity for an additional 1 week (arugula) or 4 weeks (escarole) before harvesting.

In preliminary testing, arugula plants were bolting and no longer edible when harvested after 4 weeks of Pt NP exposure (Fig. S3†). A comparison between the leaf and root Pt concentrations in arugula plants harvested after 1 week (when the plants reached peak growth) *versus* 4 weeks after foliar exposure (50 mg Pt NPs per L) showed no statistical differences (Mann–Whitney test; $n = 3$, 5 plants per replicate, $p < 0.05$; Table S1†). A similar comparison with root-exposed arugula plants, however, showed significantly higher root Pt concentrations and significantly lower leaf Pt concentrations among plants harvested 4 weeks after exposure (Mann–Whitney test; $n = 2$, 5 plants per replicate, $p < 0.05$; Table S1†). Since the main focus of this article is on foliar exposure, where no significant differences in arugula leaf and root Pt concentrations were detected with exposure time, the decision was made to harvest them after 1 week of exposure to reflect their lifecycle and appearance when normally consumed.

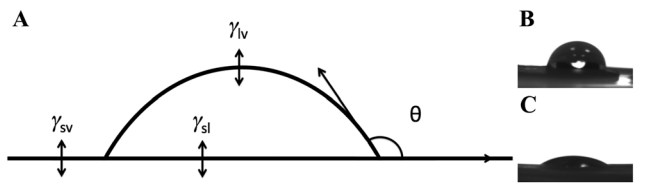

Fig. 1 Diagram representing the four variables in Young's equation as exhibited in the case of a liquid droplet on a flat, solid surface (A), along with characteristic images of water droplets on arugula (B) and escarole (C) obtained with an optical tensiometer.

2.5 Pt NP adsorption patterns on foliar surfaces

Nanoparticle adsorption patterns on foliar surfaces were investigated using SEM-EDX. Leaf samples were lyophilized at −50 °C and 0.2 mbar for 48 h before being mounted on a sample holder with double-sided carbon tape and sputter coated with ~10 nm Au. Samples were analyzed at 15 kV under ultra-high vacuum conditions (9.6×10^{-5} Pa) in secondary electron mode. Analysis with EDX was carried out on individual spots of interest.

2.6 Surface free energy theory and determination

Surface free energy (SFE) is a quantitative measure of polar and dispersive forces which determine hydrophobicity/hydrophilicity (*i.e.* wettability). The foliar SFE of plants is dictated by the degree of surface roughness (*i.e.* wrinkling and the presence of nano- and microstructures, which are positively correlated with hydrophobicity) and the chemical and structural composition of the cuticle covering the foliar surface (consisting mostly of cutin, with lower amounts of waxes, phenolics, and polysaccharides). The surface tension of a liquid droplet in combination with the foliar SFE determines the strength of adhesion (*i.e.* the contact area), which in turn affects internalization.[32,38]

Surface free energy is often estimated using indirect methods which consider the case of liquid droplets from 2 or 3 liquids of different polarities on the solid surface of interest. The contact angle, θ, formed between the liquid–vapor interface and the solid surface is related to the surface tension of the solid (SFE) by Young's equation:

$$\gamma_{sv} = \gamma_{sl} + \gamma_{lv}\cos\theta \quad (1)$$

in which γ_{sv} is the solid–vapor interfacial tension, γ_{sl} is the solid–liquid interfacial tension between the solid and the liquid droplet, and γ_{lv} is the liquid–vapor interfacial tension, or surface tension of the liquid droplet (Fig. 1).[39,40] Since the equation contains an additional unknown variable: γ_{sl}, different variations of Young's equation have been developed to deal with this issue.[41]

Following the suggestion of Fernández and Khayet,[33] the 3-liquid acid–base theory method (the Lifshitz–van der Waals-acid–base, or van Oss, Good and Chaudhury method) was used to calculate the SFE values of the plant foliar surfaces[41] (refer to the Materials and methods section and eqn (S1)–(S4) in the ESI† for additional SFE and solubility parameter calculation methods used in this work). Acid–base theory treats surface tension as the sum of Lifshitz–van der Waals forces (LW: "apolar" or dispersive forces, including London dispersion forces, Keesom dipole–dipole forces, and Debye dipole-induced dipole forces) and acid–base (AB: "polar" force) components:

$$\gamma_{lv}\left(1+\cos\theta\right) = 2\left(\sqrt{\gamma_s^d\gamma_l^d} + \sqrt{\gamma_s^+\gamma_l^-} + \sqrt{\gamma_s^-\gamma_l^+}\right) \quad (2)$$

where γ_s^d and γ_l^d, γ_s^+ and γ_l^+, and γ_s^- and γ_l^- represent the dispersive, electron-acceptor, and electron-donor components of the solid and liquid, respectively. Surface free energy is represented by $\gamma_{lv}(1 + \cos\theta)$ by treating it as the sum of the solid and liquid facial tensions minus the work of adhesion.[41] By using one apolar liquid and two polar liquids with known γ_l^d, γ_l^-, and γ_l^+ values, it is possible to determine the LW, or dispersive, and AB surface tension components of the solid.[42]

Surface free energy values were calculated using acid–base theory (eqn (2)) for the abaxial and adaxial foliar surfaces of both test plants applying recommendations and mean liquid surface tension values provided by Fernández and Khayet.[33] Static contact angle measurements were obtained by applying droplets of ultrapure water, diiodomethane (99% Sigma-Aldrich, Germany), and glycerol (99+%, Alfa Aesar, USA; 5 repetitions each) with a pipette to the foliar surfaces of the test plants. Droplet images were obtained within 10 s of droplet application and measured using a Theta Lite T101 optical tensiometer (Attension, Biolin Scientific, Finland) connected to a computer with Attension Theta software. Contact angle measurements were made for unexposed and exposed leaves at all exposure concentrations after each day of application to compare the daily and cumulative effects of foliar exposure to Pt NPs on SFE. Due to the separate locations of the tensiometer and plant chamber, leaves were detached for transport and analysis. To minimize potential variations from leaf to leaf, contact angle measurements were obtained from at least 4 leaves for each plant surface and exposure condition. In a separate analysis, the effect of aging on the abaxial and adaxial foliar SFE of both plants was found to be negligible (*i.e.* over a 10 day period, the difference was no greater than 4.11 mJ m^{-2}; Table S2†).

2.7 Pt concentrations in plant leaves and roots

Sample preparation was based on procedures used by Kroflič *et al.*[43] During harvesting, fresh roots and leaves were separated, washed, weighed, and frozen until further preparation. Minor amounts of yellowed and rotten leaves (from normal aging) in control and exposed plants were discarded. Leaves were washed in accordance with U.S. Food and Drug Administration[44] and European Food Safety Authority[45] recommendations for home produce preparation: 30 s under cool running tap water, followed by two consecutive baths in ultrapure water for 1 min each.[11] Samples of the wash water were analyzed with ICP-MS to check for the presence of Pt. Roots were thoroughly washed under cool running tap water and rinsed with ultrapure water. Plant tissues were then stored in a freezer at −20 °C until lyophilization at −50 °C and 0.2 mbar for 48 h. Leaf samples were finely milled with a Fritsch planetary micro mill Pulverisette 7 (Fritsch GmbH, Idar-Oberstein, Germany) and root samples were cut into small (~5 mm) pieces.

Approximately 0.3 g of leaf material or 0.15 g of root material were mineralized in closed Teflon tubes with 4 mL 65% HNO_3 (Suprapur, Merck, Germany) and 0.1 mL HF (Suprapur, Merck, Germany) in a Milestone UltraWAVE microwave digester (Milestone Inc., USA). Samples were heated to 220 °C at 100.0 bar (1500 W) over 20 min, maintained under these conditions for a further 15 min (1500 W), and then cooled back to room temperature over a 30 min period. Samples were diluted to 30 mL with ultrapure water. Each sample was prepared in triplicate. Blanks prepared in the same way as samples were included in each run.

Measurement of the Pt concentration in the digested samples was made by ICP-MS. The isotope measured was ^{195}Pt and external calibration was used for quantification.

Calibration standards were prepared by dilution of 1000 mg L^{-1} Pt solution (Merck, Germany). To evaluate the efficiency of the analytical procedure used, samples of leaves and roots from both plants were spiked with a known amount of Pt solution before digestion. Analysis of the Pt content following digestion showed that the recovery was 95% ± 9% (mean ± standard deviation [SD], n = 6). The limit of detection for Pt was 1.1 μg L^{-1}.

2.8 Statistical analysis

Differences in Pt concentrations in different plant segments (leaves and roots; n = 3), proportion of open stomata on foliar surfaces (n = 10), leaf mass (n = 3), and dissolved Pt concentrations between samples treated by ultracentrifugation and ultrafiltration (n = 3) were ascertained using the Mann–Whitney test at the $p < 0.05$ significance level. Foliar SFE differences between the abaxial and adaxial surfaces of arugula and escarole as a function of foliar Pt NP exposure were analyzed using a paired t-test (n = 5) at the $p < 0.05$ significance level. Normality of the data was tested with the Shapiro–Wilk test and homoscedasticity of the variance was determined using Levene's test.[46] All analyses were completed using OriginPro 2015 software.

3. Results

3.1 Pt NP characterization

Examination by SEM (Fig. S4A†) and TEM (Fig. 2A) showed that the Pt NPs were spherical in shape. Measurements of 300 randomly selected Pt NPs in the TEM image with ImageJ software indicated an average particle size of 13.4 ± 6.7 nm and a size distribution from 3.1–55.6 nm. The specific surface area measured with BET analysis was 10.65 m^2 g^{-1} Pt NPs and the chemical identity of the Pt NPs was confirmed using EDX (Fig. S4B†).

In aqueous dispersion, Pt NPs had an average hydrodynamic diameter of 121.6 ± 1.4 nm with an average polydispersity index of 0.149 ± 0.03, as obtained from triplicate DLS measurements. The zeta potential of the dispersions was measured throughout the pH range, but the point of zero charge was not reached (Fig. 2B).

3.2 Pt NP dissolution

The total concentrations of Pt detected in the acidified experimental Pt NP dispersions were in excellent agreement with the nominal values, exhibiting ≤3.0% deviation (Table 1). Concentrations of dissolved Pt in the supernatant of samples treated by ultracentrifugation and ultrafiltration were extremely low, confirming reports from the literature that Pt NPs barely dissolve.[7,47] However, the supernatant of ultracentrifuged samples contained higher concentrations of dissolved Pt compared to the supernatant of ultrafiltered samples (Table 1). These results are consistent with the fact that dissolved metal concentrations tend to be overestimated in ultracentrifuged samples due to the difficulty of removing the liquid supernatant containing the dissolved metal ion fraction without re-suspending some of the sediment particles. Conversely, dissolved metal concentrations tend to be underestimated in ultrafiltered samples due to the adsorption of metal ions onto the filter.[48] Nonetheless, statistical differences were not detected when dissolved Pt concentrations measured in ultracentrifuged and ultrafiltered samples were compared (Mann–Whitney test, n = 3, $p < 0.05$).

The concentrations of dissolved Pt ions in the supernatant of samples containing Pt NPs with either arugula or escarole

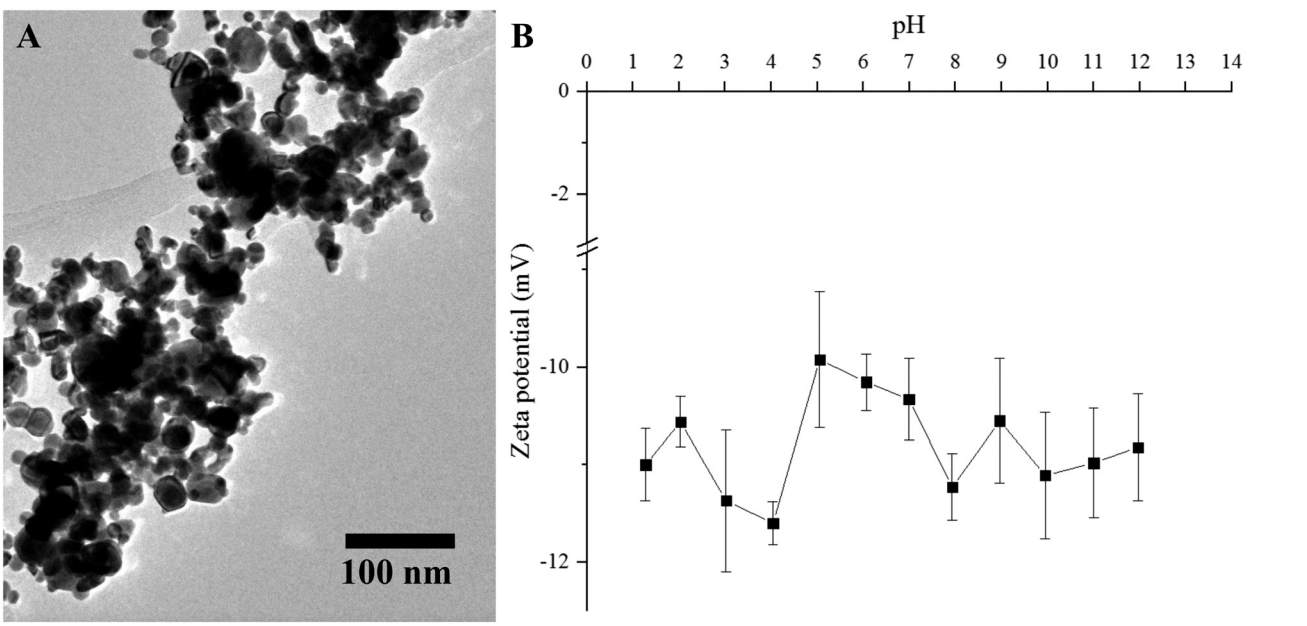

Fig. 2 TEM micrograph of Pt NPs (A) and graph depicting the zeta potential of Pt NPs dispersed in ultrapure water (50 mg L^{-1}) across the pH scale (B). Error bars represent standard error (n = 5).

Table 1 Pt NP experimental concentrations and dissolution

Sample	Nominal Pt concentration (mg L^{-1})	Total measured Pt concentration (mg L^{-1})	Pt concentration in supernatant after ultracentrifugation (μg L^{-1})	Pt concentration in supernatant after ultrafiltration (μg L^{-1})	Dissolved Pt fraction (%) with corresponding Pt concentration in supernatant (in parentheses)[a]
Pt NPs	5	5.019 ± 0.073	2.070 ± 0.412	0.178 ± 0.022	0.041 ± 0.008 (2.070 ± 0.412)
	50	50.409 ± 0.914	5.993 ± 0.413	1.718 ± 0.063	0.012 ± 0.001 (5.993 ± 0.413)
	500	514.485 ± 11.055	36.277 ± 6.160	19.145 ± 5.523	0.007 ± 0.001 (36.277 ± 6.160)
Pt NPs and arugula	5	5.019 ± 0.073	—	0.709 ± 0.044	0.014 ± 0.001 (0.709 ± 0.044)
Pt NPs and escarole	5	5.019 ± 0.073	—	0.457 ± 0.005	0.009 ± 0.000 (0.457 ± 0.005)

All data are mean ± SD (n = 3). [a] The dissolved Pt fraction (%) is provided in terms of ultracentrifugation in the cases of Pt NPs dispersed in water (5, 50, and 500 mg L^{-1}) and in terms of ultrafiltration in the cases of Pt NPs and arugula and Pt NPs and escarole.

leaves were approximately 4.0 and 2.6 times greater, respectively, than the corresponding concentration of dissolved Pt measured in the bare dispersion treated by ultrafiltration (the mean leaf mass ± SD was 0.243 ± 0.022 g arugula and 0.156 ± 0.026 g escarole; Table 1). Due to incomplete sedimentation of the samples treated by ultracentrifugation and the frothy appearance of the liquid after filtration, only samples treated by ultrafiltration were analyzed to avoid measurement discrepancies (Fig. S1†).

3.3 Leaf surface characteristics and Pt NP surface adsorption patterns

Image analysis of unexposed, lyophilized arugula and escarole leaf samples (Fig. 3A and B, respectively) revealed a low degree of surface roughness with similar stomatal densities between the two plants and between abaxial and adaxial surfaces: arugula abaxial surface: 107.0 ± 2.3 stomata per mm^2; arugula adaxial surface: 85.6 ± 15.9 stomata per mm^2; escarole abaxial surface: 98.6 ± 7.6 stomata per mm^2; escarole adaxial surface: 69.5 ± 9.9 stomata per mm^2. Escarole was found to contain low numbers of trichomes on the abaxial (4.6 ± 3.6 trichomes per mm^2) and adaxial (1.1 ± 2.4 trichomes per mm^2) surfaces whereas no trichomes were found on arugula foliar surfaces. Statistical means comparison to determine changes in the proportion of open stomata with foliar exposure to 500 mg Pt NPs per L (Mann–Whitney test, n = 10, $p < 0.05$) indicated decreases in the proportion of open stomata for abaxial and adaxial arugula surfaces (no open stomata were found), a significant increase for escarole abaxial surfaces, and no difference for escarole adaxial surfaces (Table S3 and Fig. S5†).

Observation with SEM did not show any differences in the Pt NP adsorption patterns between the abaxial and adaxial foliar surfaces of each plant; however, clear differences were observed between arugula and escarole leaves exposed to the 500 mg L^{-1} dispersion over a 5 day exposure period (Fig. 3C and D, with EDX spectra confirming the presence of Pt on both plants presented in Fig. 3E and F for arugula and escarole, respectively). While Pt NPs on escarole foliar surfaces (Fig. 3D) were agglomerated into discontinuous islands of Pt nano- and microparticles, on arugula they appeared as a nearly unbroken sheet of highly aggregated/agglomerated particles (Fig. 3C). Similarly, the magnified images of stomata showed relatively low amounts of Pt NPs around escarole stomata, primarily as loose agglomerates (insert in Fig. 3D), whereas relatively large amounts of Pt NPs were caked around the stomata of arugula as loosely bound agglomerates and tightly bound aggregates (insert in Fig. 3C). The appearance of the Pt NPs on arugula leaf surfaces was consistent with the fact that water droplets do not spread out over surfaces with low SFE, and hence the Pt NPs on arugula were concentrated over a smaller surface area relative to Pt NPs on escarole.

None of the exposed leaves exhibited necrosis in response to Pt NP exposure (Fig. S6†). However, means comparison of the leaf masses from control and exposed plants (Mann–Whitney test, n = 3, $p < 0.05$) showed that the mass of 500 mg Pt NPs per L foliar-exposed arugula leaves was significantly lower than the leaf mass from the other arugula groups (5 and 50 mg Pt NPs per L foliar-exposed, root-exposed, and control groups), and that the mass of root-exposed arugula leaves was significantly higher than that of the other arugula groups (*i.e.* 5, 50, and 500 mg Pt NPs per L foliar-exposed and control groups; Table S4†).

3.4 Surface free energy response to Pt NP exposure

Graphical representations with trend lines depicting abaxial and adaxial foliar SFE (acid–base theory) in response to 500 mg Pt NPs per L exposure for both plants are displayed in Fig. 4 while graphical representations with trend lines depicting abaxial and adaxial foliar SFE in response to 5 and 50 mg Pt NPs per L exposures are shown in Fig. S7.† Contact angle values are available in Table S5† while full numerical SFE results are available in Table S6.† Comparing the two plants before the exposure period, arugula foliar surfaces had substantially lower SFE values (Fig. 4A; abaxial: 36.47 mJ m^{-2}; Fig. 4B; adaxial: 39.12 mJ m^{-2}) than the foliar surfaces of escarole (Fig. 4C; abaxial: 143.91 mJ m^{-2}; Fig. 4D; adaxial: 67.07 mJ m^{-2}). Although there was poor linearity of SFE with exposure to the Pt NP dispersion, efforts were still made to evaluate possible relationships between the two factors since, at least in the cases of the arugula abaxial and escarole adaxial surfaces (Fig. 4A and D, respectively) SFE changed noticeably with each day of exposure.

Examination of the graph trend lines in Fig. 4 shows that the arugula abaxial foliar surface showed the greatest overall change in SFE from Pt NP exposure, displaying an overall increase of 81.4 mJ m^{-2}, or a more than two-fold increase over

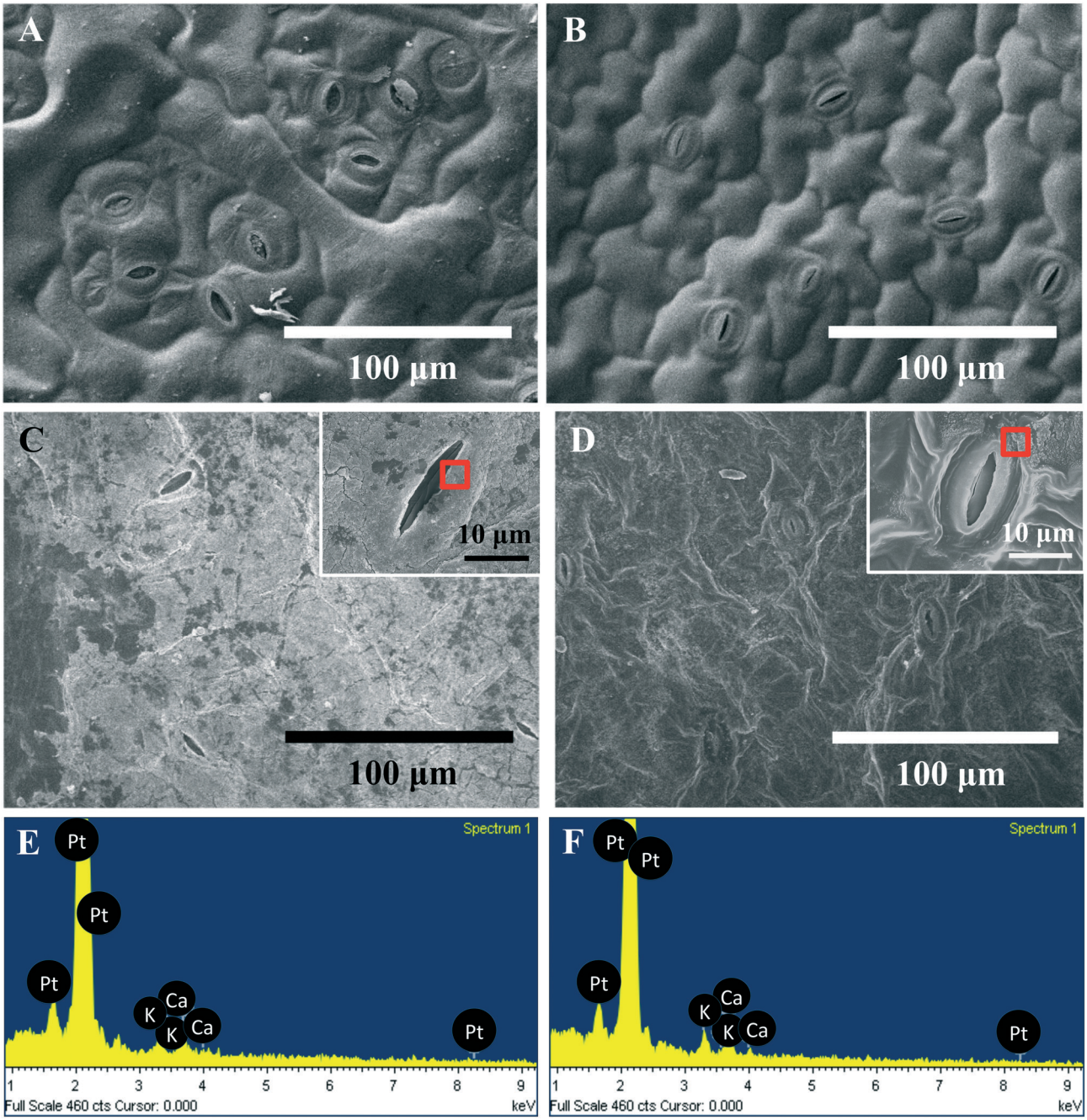

Fig. 3 SEM micrographs showing the abaxial foliar surfaces of control (A and B) and 500 mg Pt NPs per L foliar-exposed arugula and escarole, respectively, with the magnified stomata presented as inserts (C and D). EDX spectra (E and F; arugula and escarole, respectively) for the red-boxed areas (inserts in C and D) on exposed leaves confirm the presence of Pt NPs, which appear as white particles.

the exposure period (Fig. 4A). The adaxial surface of escarole showed a similar, but comparatively modest overall increase of 17.4 mJ m^{-2} over the exposure period (Fig. 4D). Both the arugula adaxial and escarole abaxial foliar surfaces displayed a slight decreasing trend in SFE (overall decrease of 6.8 and 22.1 mJ m^{-2} for arugula [Fig. 4B] and escarole [Fig. 4C], respectively). Statistical analysis to compare the abaxial and adaxial foliar surfaces of arugula and escarole over the course of the Pt NP exposure period showed that the abaxial surfaces of arugula and escarole (Fig. 4A and C, respectively) were not significantly different, whereas the adaxial surfaces of arugula and escarole (Fig. 4B and D, respectively) were significantly different (paired *t*-test, $n = 5$, $p < 0.05$).

3.5 Concentrations of translocated Pt in exposed and unexposed plant segments

The Pt concentrations measured in the leaves and roots, along with the average fractions (%) of total Pt detected in leaf and root segments of the treated plants are presented in

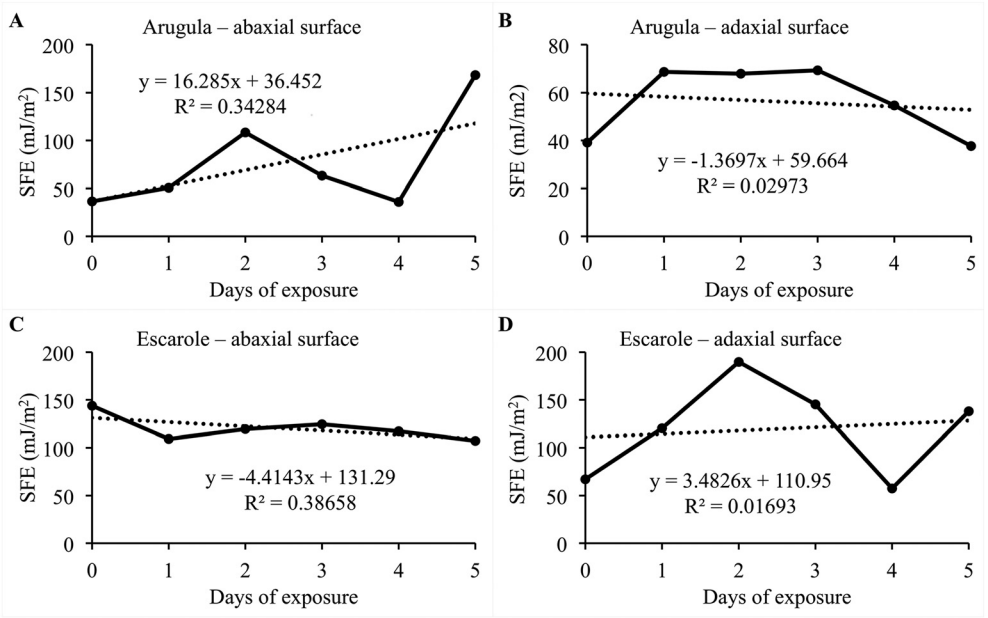

Fig. 4 SFE values accompanied by trend lines for abaxial (A and C) and adaxial (B and D) foliar surfaces of arugula and escarole, respectively, before the exposure period and following each day of foliar treatment to 500 mg Pt NPs per L dispersion.

Fig. 5A and B, respectively. Numeric Pt concentration values and total, leaf, and root Pt quantities are provided in Tables S7 and S8,† respectively. Control leaves and roots from both plants contained extremely low levels of Pt (mean values of <3.5 ng g^{-1} dry weight [DW]); therefore it could be assumed that Pt detected in samples from the treatment groups originated from the experimental exposures.

Arugula leaves consistently contained statistically higher Pt concentrations than escarole leaves at all Pt NP exposures (approximately 33, 31, and 14 times higher, on average, for the 5, 50, and 500 mg Pt NPs per L foliar exposures, respectively, and 12 times higher, on average, for the root exposure). This indicated both a higher capacity to retain foliar applications of Pt NPs and to internalize and translocate root-applied Pt NPs from roots to leaves (Fig. 5A). In the case of foliar applications, the low SFE of the arugula leaves meant that applied droplets of Pt NP dispersion remained attached to the leaf surface without spreading out and dripping towards the bottom of the leaves as was the case with escarole. The amount of Pt detected in water samples from the washing procedure was negligible (<0.15 ng mL^{-1}), showing that Pt NPs were not removed from either plant by the washing procedure used in this study.

Root Pt concentrations increased in a linear manner with increasing concentration of the foliar Pt NP application, reaching statistical increases from controls at 50 and 500 mg Pt NPs per L. At 5 mg Pt NPs per L foliar exposure, only escarole roots contained statistically elevated Pt concentrations relative to the controls. Among root samples, escarole consistently accumulated higher Pt concentrations than arugula (approximately 17, 6, 4, and 3 times higher, on average, for the root and 5, 50, and 500 mg Pt NPs per L foliar exposures, respectively; Fig. 5B and Table S7†).

Because the total fraction of translocated Pt from leaves to roots was extremely low for both plants ($<1\%$), an attempt was made to assess whether Pt internalization and translocation from leaves to roots might have occurred only in the dissolved form by comparing the average fractions of total Pt measured in the roots (Fig. 5B; *i.e.* translocated Pt) with the corresponding fractions of dissolved Pt measured in samples prepared by ultracentrifugation (Table 1). Size is considered to be the main determinant of NP passage into plant tissues.[49] Therefore, there are two potential uptake mechanisms. Assuming that the total fraction of dissolved Pt would be internalized and translocated by the leaf tissue due to the lack of a size exclusion barrier over the entire plant surface, any fraction of translocated Pt above the dissolved fraction might be further assumed to have been internalized and translocated in the NP form. Since the average fraction of translocated Pt in escarole was many orders of magnitude higher than the fractions of dissolved Pt, this could indicate that the escarole plants may have been able to internalize and translocate the Pt as NPs. It is also possible that the escarole foliar surface environment (*e.g.* temperature, humidity, and microbial communities) is more conducive to Pt NP dissolution,[11] and that dissolved Pt uptake generates a higher rate of dissolution on the foliar surface.[50]

By contrast, the average fractions of total Pt measured in the roots of foliar-exposed arugula plants (Fig. 5B) were several orders of magnitude lower than the corresponding fractions of dissolved Pt (Table 1). In the absence of suitable methods to accurately locate and characterize the elements present at such low concentrations in plant tissues, it is therefore not possible to rule out the possibility that Pt was internalized and translocated to roots only in its dissolved

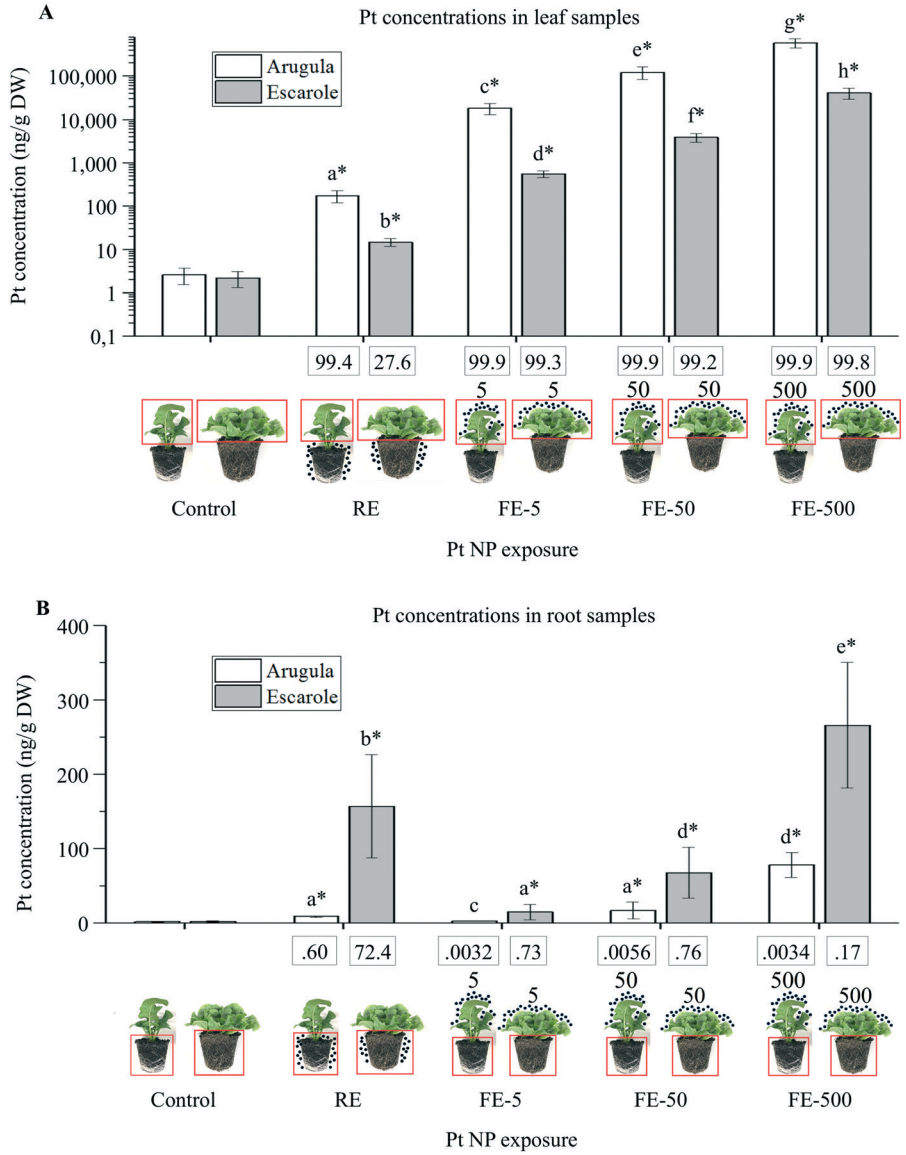

Fig. 5 Pt concentrations of arugula and escarole leaves (A) and roots (B) after Pt NP foliar exposure (FE) or root exposure (RE). Significant mean differences between exposure groups are indicated by different letters, while letters in common indicate a lack of difference. An asterisk indicates a statistical difference between an exposure group and the corresponding control group ($p < 0.05$). Images denote plant type (arugula: left; escarole: right), analyzed plant segment (red box), and Pt NP exposure (black dots on roots or leaves with concentration of foliar exposure in mg L^{-1}). Boxed numbers above sample images indicate the mean fraction of total Pt (%) in the sample calculated from each replicate of the exposure. DW = dry weight.

form. These findings therefore illustrate different surface responses to foliar Pt NP exposure between the two plants.

The root-exposed leaf samples from both plants showed very high percentages of Pt NP uptake and translocation from roots to leaves (Fig. 5A and Table S4†). In arugula, nearly the entire amount of Pt was present in the leaves (99.4%) whereas in escarole, the percentage of Pt in leaves was markedly lower (27.6%). Had the arugula plants been harvested after 4 weeks of exposure, we would have expected to measure similar leaf and root Pt concentrations to those in escarole (Table S1†). The soil pH of Pt NP exposed plants at harvest was not statistically different from that of the controls (Table S9†).

4. Discussion

The uptake and translocation of Pt from leaves to roots and from roots to leaves was successfully confirmed in two plant species: arugula and escarole. The two species exhibited different responses in terms of Pt NP surface adsorption and Pt translocation from leaves to roots. This could partly be related to the different surface free energy (SFE) of the two plant species.

Among arugula leaves, which have low SFE, a higher amount of material was adsorbed onto the leaf surfaces (14–33 times higher Pt concentrations were detected than in escarole leaves), the stomata were closed, and less Pt was

detected in roots when compared to escarole. The closed stomata on arugula leaves were likely the result of shading effects, which occur when the amount of light reaching the surface is insufficient for photosynthesis to occur.[51] Although this was not tested by removing Pt NPs to examine whether the stomata would reopen, the finding of significantly lower arugula leaf mass after foliar exposure to 500 mg Pt NPs per L in comparison to the other arugula groups is consistent with a decreased ability to synthesize the carbohydrates needed for optimal growth. Additional examination of the arugula leaf samples foliar-exposed to 50 mg Pt NPs per L by SEM-EDX showed that while the stomata were closed in areas with concentrated Pt NPs, open stomata were still visible in areas of the leaf where Pt NPs were not present. A comparison of the proportion of open stomata in these areas with the proportion of open stomata on unexposed leaves showed a significant decrease (Mann–Whitney test, $n = 10$, $p < 0.05$; Table S10†). This suggests a partial shading effect at 50 mg Pt NPs per L foliar exposure and the existence of a full shading effect at 500 mg Pt NPs per L foliar exposure.

In escarole leaves, which have high SFE, less Pt was adsorbed onto the surfaces, the stomata remained open, and higher Pt concentrations were measured in roots. The high SFE could directly enhance Pt NP internalization through the formation of water film connections between the inner and outer portions of the leaves, which has been associated with an increased capacity for particle uptake by stomata.[30] This relationship between the cuticular structure (*i.e.* the relative proportions of the cuticular constituents and the chemical bonding between them), foliar SFE, and water film formation aligns with the cuticle's major physiological role in regulating water balance.[38] Although foliar SFE may change with repeated particle exposure, our findings were in agreement with similar studies[52,53] which demonstrated inconsistent changes with regard to whether it increased or decreased. There were no statistical differences in leaf mass between the different escarole groups.

In our study, less than 1% of the total Pt was detected in the roots of foliar-exposed plants. In arugula, we have explained that the fraction of translocated Pt from leaves to roots could originate from dissolved Pt NPs. The average dissolution of Pt NPs in ultrapure water was several orders of magnitude greater than the average percentage of Pt translocated to roots by arugula. Consequently, the dissolved fraction of Pt is sufficient to explain the amount present in roots. In escarole, the amount of Pt detected in roots may not have been due entirely to dissolved Pt NPs, because the fraction of translocated Pt was many orders of magnitude higher than the potentially dissolved Pt from the Pt NP dispersions. However, the escarole foliar surface environment and the rate of uptake of dissolved Pt may have favored the dissolution of Pt NPs relative to arugula.[11,50] In some cases, foliar uptake has been attributed to the interactions between the particle and leaf surface, resulting in enhanced bioavailability through the formation of organic coatings[37,54] and secondary species.[27] Within short time periods (60 days), elemental Pt is highly unreactive even in its particulate form;[47] therefore it is unlikely that higher uptake by escarole could be explained by processes other than dissolution. An attempt to locate Pt NPs within arugula and escarole leaves using SEM (with leaf cross sections) and focused ion beam-SEM yielded no signs of Pt uptake in its particulate form. Here, analysis of xylem and/or phloem sap by electron microscopy and ICP-MS could have provided better insight into the form of Pt and its uptake mechanisms by the foliar surfaces. In either case, the finding of increased Pt translocation, whether as NPs or in its dissolved form, is in line with the high SFE of the escarole leaves. It has been previously reported that the foliar uptake of NPs occurs mainly through a hydrophilic pathway consisting of stomata.[11,30,37,54,55] Internalized NPs may reach the phloem, enabling transport to roots.[56] Wang *et al.*[23] showed that 1.23% of the foliar-applied, non-dissolvable TiO_2 NPs were translocated to roots in watermelon. This is in agreement with our findings in the case of escarole, but not for arugula.

Platinum NP uptake and translocation from roots to leaves was also confirmed. Root to leaf NP uptake and translocation occurs when NPs are taken up with water and nutrients through the xylem *via* passage through the epidermis, cortex, Casparian strip (*via* the symplasmic pathway) and stele. Plant transpiration provides the driving force for their movement from roots to stems and leaves.[57,58] Because the plants were cultivated in soil rather than hydroponics systems, our results provide a realistic root exposure scenario. Although the fraction of root-to-leaf translocation was much higher than that of leaf-to-root translocation (nearly 30 000 times higher for arugula and 160 times higher for escarole), the soil matrix provides a barrier to NP exposure which is absent for above-ground plant segments.

Our study showed that Pt NPs were not removed from the plants when washed only with water, indicating that they are most likely to remain adhered to and within above-ground plant segments under this washing regime. Insignificant NP removal from foliar surfaces has been frequently observed, including in the case of maize leaf exposure to CeO_2 NPs,[59] lettuce leaf exposure to Ag NPs,[37] and grapevine leaf exposure to poly(lactic-*co*-glycolic) acid NPs.[60] During industrial processing or home preparation, produce may be exposed to chlorine[61] or other additives in wash water, which could potentially affect NP attachment/detachment differently than water alone. For example, Hong *et al.*[24] found enhanced removal of CeO_2 NPs from cucumber leaves after washing with 10 mM $CaCl_2$ solution (81.0% ± 1.0% removal) in comparison to washing only with water (73.0% ± 7.5% removal). However to the best of our knowledge, there have been no studies focused exclusively on investigating strategies for NP removal from plant surfaces.

Our results have implications for food safety showing that foliar exposure to Pt NPs leads to significant adhesion and contamination of arugula and escarole leaves, and that low SFE significantly increases the extent of Pt NP retention. In light of other reports showing the disproportionate influence

of urban and industrial air pollution on above-ground plant contamination,[10–13] these findings further suggest the need to include air quality as a factor in discussions of food safety and urban gardening. Since NPs are not removed by washing only with water, strategies to limit human consumption of metallic NPs from atmospheric deposits and agricultural foliar sprays should focus on the removal of outer peels and leaves and implementation of physical barriers, such as the use of greenhouses and the cultivation of tall bushes and trees on garden perimeters.[62] Because SFE affects NP retention, we could expect the risk of consuming urban-grown foods to be lower for plants with higher SFE. In addition, our results contribute to the expectation that nanoformulated plant treatments could be successfully applied to roots or leaves with minimal risk of environmental transfer.

5. Conclusions

Our results showed that arugula and escarole internalized and translocated Pt from leaves to roots and from roots to leaves. The root-to-leaf pathway was more significant in terms of the fraction of internalized and translocated Pt NPs. For the first time, we showed the role of foliar SFE in the capacity to retain the applied Pt NP dispersion, with consequences for Pt NP aggregation/agglomeration and uptake and translocation to roots. Arugula leaves have low SFE and contained Pt NPs at greater concentrations and in a more highly aggregated/agglomerated state than on escarole leaves. This further resulted in likely shading effects and complete stomata closure, with significantly lower Pt translocation to roots compared to escarole. Because these results carry implications for food and environmental safety and the use of agricultural nanotechnologies, further studies are needed to assess the foliar uptake and translocation behaviors of other plants and to develop new strategies for preventing and reducing NP exposure and retention by above-ground plant surfaces.

Conflicts of interest

There are no conflicts to declare.

Acknowledgements

This work has been financed and supported by the ISO-FOOD Project "ERA Chair for Isotope Techniques in Food Quality, Safety and Traceability" (grant agreement No. 621329). Many thanks go to Prof. Dr. M. Horvat and Prof. Dr. R. Milačič for their expert advice during the planning phase of this study. We would also like to thank Prof. Dr. M. Kranjc for support with SFE calculation, Asst. Prof. dr. S. Škapin for BET analysis of the Pt nanoparticles, and Marta Jagodic for assistance with ICP-MS trouble-shooting and measurement. Additional acknowledgement for technical advice and assistance go to Monika Kos, Luka Pirker, Tome Eftimov, Maja Koblar, Dr. Martina Lorenzetti, and Alenka Malovrh.

References

1 S. C. C. Arruda, A. L. D. Silva, R. M. Galazzi, R. A. Azevedo and M. A. Z. Arruda, Nanoparticles Applied to Plant Science: A Review, *Talanta*, 2015, **131**, 693–705.
2 P. Miralles, T. L. Church and A. T. Harris, Toxicity, Uptake, and Translocation of Engineered Nanomaterials in Vascular Plants, *Environ. Sci. Technol.*, 2012, **46**(17), 9224–9239.
3 M. Moustafa, A. Mohamed, A.-R. Ahmed and H. Nazmy, Mass Size Distributions of Elemental Aerosols in Industrial Area, *J. Adv. Res.*, 2015, **6**(6), 827–832.
4 J. Csavina, J. Field, M. P. Taylor, S. Gao, A. Landázuri, E. A. Betterton and A. E. Sáez, A Review on the Importance of Metals and Metalloids in Atmospheric Dust and Aerosol from Mining Operations, *Sci. Total Environ.*, 2012, **433**, 58–73.
5 H. Wichmann, G. A. K. Anquandah, C. Schmidt, D. Zachmann and M. A. Bahadir, Increase of Platinum Group Element Concentrations in Soils and Airborne Dust in an Urban Area in Germany, *Sci. Total Environ.*, 2007, **388**(1–3), 121–127.
6 S. Terashima, N. Mita, S. Nakao and S. Ishihara, Platinum and Palladium Abundances in Marine Sediments and Their Geochemical Behavior in Marine Environments, *Bull. Geol. Surv. Jpn.*, 2002, **53**(11/12), 725–747.
7 K. H. Ek, G. M. Morrison and S. Rauch, Environmental Routes for Platinum Group Elements to Biological Materials —a Review, *Sci. Total Environ.*, 2004, **334–335**, 21–38.
8 X. Ma, J. Geiser-Lee, Y. Deng and A. Kolmakov, Interactions between Engineered Nanoparticles (ENPs) and Plants: Phytotoxicity, Uptake and Accumulation, *Sci. Total Environ.*, 2010, **408**(16), 3053–3061.
9 C. M. Rico, S. Majumdar, M. Duarte-Gardea, J. R. Peralta-Videa and J. L. Gardea-Torresdey, Interaction of Nanoparticles with Edible Plants and Their Possible Implications in the Food Chain, *J. Agric. Food Chem.*, 2011, **59**(8), 3485–3498.
10 E. Schreck, Y. Foucault, G. Sarret, S. Sobanska, L. Cécillon, M. Castrec-Rouelle, G. Uzu and C. Dumat, Metal and Metalloid Foliar Uptake by Various Plant Species Exposed to Atmospheric Industrial Fallout: Mechanisms Involved for Lead, *Sci. Total Environ.*, 2012, **427–428**, 253–262.
11 E. Schreck, V. Dappe, G. Sarret, S. Sobanska, D. Nowak, J. Nowak, E. A. Stefaniak, V. Magnin, V. Ranieri and C. Dumat, Foliar or Root Exposures to Smelter Particles: Consequences for Lead Compartmentalization and Speciation in Plant Leaves, *Sci. Total Environ.*, 2014, **476–477**, 667–676.
12 M. S. Al Jassir, A. Shaker and M. A. Khaliq, Deposition of Heavy Metals on Green Leafy Vegerables Sold on Roadsides of Riyadh City, Saudi Arabia, *Bull. Environ. Contam. Toxicol.*, 2005, **75**(5), 1020–1027.
13 X. Hu, Y. Zhang, J. Luo, M. Xie, T. Wang and H. Lian, Accumulation and Quantitative Estimates of Airborne Lead for a Wild Plant (Aster Subulatus), *Chemosphere*, 2011, **82**(10), 1351–1357.
14 Y. Dan, W. Zhang, R. Xue, X. Ma, C. Stephan and H. Shi, Characterization of Gold Nanoparticle Uptake by Tomato

Plants Using Enzymatic Extraction Followed by Single-Particle Inductively Coupled Plasma-Mass Spectrometry Analysis, *Environ. Sci. Technol.*, 2015, **49**(5), 3007–3014.

15 C. O. Dimkpa, D. E. Latta, J. E. McLean, D. W. Britt, M. I. Boyanov and A. J. Anderson, Fate of CuO and ZnO Nano- and Microparticles in the Plant Environment, *Environ. Sci. Technol.*, 2013, **47**(9), 4734–4742.

16 J. Geisler-Lee, Q. Wang, Y. Yao, W. Zhang, M. Geisler, K. Li, Y. Huang, Y. Chen, A. Kolmakov and X. Ma, Phytotoxicity, Accumulation and Transport of Silver Nanoparticles by Arabidopsis Thaliana, *Nanotoxicology*, 2013, **7**(3), 323–337.

17 J. A. Hernandez-Viezcas, H. Castillo-Michel, J. C. Andrews, M. Cotte, C. Rico, J. R. Peralta-Videa, Y. Ge, J. H. Priester, P. A. Holden and J. L. Gardea-Torresdey, In Situ Synchrotron X-Ray Fluorescence Mapping and Speciation of CeO2 and ZnO Nanoparticles in Soil Cultivated Soybean (Glycine Max), *ACS Nano*, 2013, **7**(2), 1415–1423.

18 J. Koelmel, T. Leland, H. Wang, D. Amarasiriwardena and B. Xing, Investigation of Gold Nanoparticles Uptake and Their Tissue Level Distribution in Rice Plants by Laser Ablation-Inductively Coupled-Mass Spectrometry, *Environ. Pollut.*, 2013, **174**, 222–228.

19 X. Ma, A. Gurung and Y. Deng, Phytotoxicity and Uptake of Nanoscale Zero-Valent Iron (NZVI) by Two Plant Species, *Sci. Total Environ.*, 2013, **443**, 844–849.

20 A. D. Servin, M. I. Morales, H. Castillo-Michel, J. A. Hernandez-Viezcas, B. Munoz, L. Zhao, J. E. Nunez, J. R. Peralta-Videa and J. L. Gardea-Torresdey, Synchrotron Verification of TiO2 Accumulation in Cucumber Fruit: A Possible Pathway of TiO2 Nanoparticle Transfer from Soil into the Food Chain, *Environ. Sci. Technol.*, 2013, **47**(20), 11592–11598.

21 J. Wang, Y. Yang, H. Zhu, J. Braam, J. L. Schnoor and P. J. J. Alvarez, Uptake, Translocation, and Transformation of Quantum Dots with Cationic versus Anionic Coatings by Populus Deltoides × Nigra Cuttings, *Environ. Sci. Technol.*, 2014, **48**(12), 6754–6762.

22 G. Zhai, K. S. Walters, D. W. Peate, P. J. J. Alvarez and J. L. Schnoor, Transport of Gold Nanoparticles through Plasmodesmata and Precipitation of Gold Ions in Woody Poplar, *Environ. Sci. Technol. Lett.*, 2014, **1**(2), 146–151.

23 W.-N. Wang, J. C. Tarafdar and P. Biswas, Nanoparticle Synthesis and Delivery by an Aerosol Route for Watermelon Plant Foliar Uptake, *J. Nanopart. Res.*, 2013, **15**(1), 1417.

24 J. Hong, J. R. Peralta-Videa, C. Rico, S. Sahi, M. N. Viveros, J. Bartonjo, L. Zhao and J. L. Gardea-Torresdey, Evidence of Translocation and Physiological Impacts of Foliar Applied CeO2 Nanoparticles on Cucumber (Cucumis Sativus) Plants, *Environ. Sci. Technol.*, 2014, **48**(8), 4376–4385.

25 J. Hong, L. Wang, Y. Sun, L. Zhao, G. Niu, W. Tan, C. M. Rico, J. R. Peralta-Videa and J. L. Gardea-Torresdey, Foliar Applied Nanoscale and Microscale CeO2 and CuO Alter Cucumber (Cucumis Sativus) Fruit Quality, *Sci. Total Environ.*, 2016, **563–564**, 904–911.

26 L. Zhao, Q. Hu, Y. Huang, A. N. Fulton, C. Hannah-Bick, A. S. Adeleye and A. A. Keller, Activation of Antioxidant and Detoxification Gene Expression in Cucumber Plants Exposed to a Cu(OH)2 Nanopesticide. Environ. Sci, *Nano*, 2017, **4**(8), 1750–1760.

27 T. Xiong, C. Dumat, V. Dappe, H. Vezin, E. Schreck, M. Shahid, A. Pierart and S. Sobanska, Copper Oxide Nanoparticle Foliar Uptake, Phytotoxicity, and Consequences for Sustainable Urban Agriculture, *Environ. Sci. Technol.*, 2017, **51**(9), 5242–5251.

28 A. Fleischer, M. A. O'Neill and R. Ehwald, The Pore Size of Non-Graminaceous Plant Cell Walls Is Rapidly Decreased by Borate Ester Cross-Linking of the Pectic Polysaccharide Rhamnogalacturonan II, *Plant Physiol.*, 1999, **121**(3), 829–838.

29 L. C. D. Silva, M. A. Oliva, A. A. Azevedo and J. M. D. Araújo, Responses of Restinga Plant Species to Pollution from an Iron Pelletization Factory, *Water, Air, Soil Pollut.*, 2006, **175**(1–4), 241–256.

30 T. Eichert, A. Kurtz, U. Steiner and H. E. Goldbach, Size Exclusion Limits and Lateral Heterogeneity of the Stomatal Foliar Uptake Pathway for Aqueous Solutes and Water-Suspended Nanoparticles, *Physiol. Plant.*, 2008, **134**(1), 151–160.

31 G. Uzu, S. Sobanska, G. Sarret, M. Muñoz and C. Dumat, Foliar Lead Uptake by Lettuce Exposed to Atmospheric Fallouts, *Environ. Sci. Technol.*, 2010, **44**(3), 1036–1042.

32 V. Fernandez and P. H. Brown, From Plant Surface to Plant Metabolism: The Uncertain Fate of Foliar-Applied Nutrients, *Front. Plant Sci.*, 2013, **4**, 289.

33 V. Fernández and M. Khayet, Evaluation of the Surface Free Energy of Plant Surfaces: Toward Standardizing the Procedure, *Front. Plant Sci.*, 2015, **6**, 510.

34 K. A. Khalik, Morphological Studies on Trichomes of Brassicaceae in Egypt and Taxonomic Significance, *Acta Bot. Croat.*, 2005, **64**(1), 57–73.

35 K. Koch, B. Bhushan and W. Barthlott, Multifunctional Surface Structures of Plants: An Inspiration for Biomimetics, *Prog. Mater. Sci.*, 2009, **54**(2), 137–178.

36 J. S. Taurozzi, V. A. Hackley and M. R. Wiesner, Ultrasonic Dispersion of Nanoparticles for Environmental, Health and Safety Assessment – Issues and Recommendations, *Nanotoxicology*, 2011, **5**(4), 711–729.

37 C. Larue, H. Castillo-Michel, S. Sobanska, L. Cécillon, S. Bureau, V. Barthès, L. Ouerdane, M. Carrière and G. Sarret, Foliar Exposure of the Crop Lactuca Sativa to Silver Nanoparticles: Evidence for Internalization and Changes in Ag Speciation, *J. Hazard. Mater.*, 2014, **264**, 98–106.

38 E. Domínguez, J. A. Heredia-Guerrero and A. Heredia, The Biophysical Design of Plant Cuticles: An Overview, *New Phytol.*, 2011, **189**(4), 938–949.

39 J. K. Spelt, D. Li and A. W. Neumann The Equation of State Approach to Interfacial Tensions, in *Modern Approaches to Wettability*, ed. M. E. Schrader and G. I. Loeb, Springer US, 1992, pp. 101–142.

40 Y. Yuan and T. R. Lee Contact Angle and Wetting Properties, in *Surface Science Techniques*, ed. G. Bracco and B. Holst, Springer Series in Surface Sciences, Springer, Berlin Heidelberg, 2013, pp. 3–34.

41 F. Hejda, P. Solar and J. Kousal *Surface Free Energy Determination by Contact Angle Measurements - A Comparison of Various Approaches*, 2010, pp. 25–30.
42 C. J. Van Oss, M. K. Chaudhury and R. J. Good, Interfacial Lifshitz-van Der Waals and Polar Interactions in Macroscopic Systems, *Chem. Rev.*, 1988, **88**(6), 927–941.
43 A. Kroflič, M. Germ, Š. Mechora and V. Stibilj, Selenium and Its Compounds in Aquatic Plant Veronica Anagallis-Aquatica, *Chemosphere*, 2016, **151**, 296–302.
44 *Food and Drug Administration: Center for Food Safety and Applied Nutrition. Produce: Selecting and Serving it Safely*, https://www.fda.gov/Food/ResourcesForYou/Consumers/ucm114299.htm (accessed Nov 16, 2017).
45 European Food Safety Authority, *EFSA Updates Consumer Advice on Sprout Consumption Following the 2011 E. coli Outbreak in Germany & France*, https://www.efsa.europa.eu/en/press/news/111003a (accessed Nov 16, 2017).
46 T. Eftimov, P. Korošec and B. Koroušić Seljak, A Novel Approach to Statistical Comparison of Meta-Heuristic Stochastic Optimization Algorithms Using Deep Statistics, *Inf. Sci.*, 2017, **417**(Supplement C), 186–215.
47 S. Lustig, S. Zang, W. Beck and P. Schramel, Dissolution of Metallic Platinum as Water Soluble Species by Naturally Occurring Complexing Agents, *Microchim. Acta*, 1998, **129**(3–4), 189–194.
48 N. Odzak, D. Kistler, R. Behra and L. Sigg, Dissolution of Metal and Metal Oxide Nanoparticles in Aqueous Media, *Environ. Pollut.*, 2014, **191**, 132–138.
49 K.-J. Dietz and S. Herth, Plant Nanotoxicology, *Trends Plant Sci.*, 2011, **16**(11), 582–589.
50 M. S. Silberberg and P. G. Amateis Kinetics: Rates and Mechanisms of Chemical Reactions, in *Chemistry: The Molecular Nature of Matter and Change*, McGraw-Hill Education, New York, NY, 2015.
51 T. Hirano, M. Kiyota and I. Aiga, Physical Effects of Dust on Leaf Physiology of Cucumber and Kidney Bean Plants, *Environ. Pollut.*, 1995, **89**(3), 255–261.
52 S. L. Honour, J. N. B. Bell, T. W. Ashenden, J. N. Cape and S. A. Power, Responses of Herbaceous Plants to Urban Air Pollution: Effects on Growth, Phenology and Leaf Surface Characteristics, *Environ. Pollut.*, 2009, **157**(4), 1279–1286.
53 F. Kardel, K. Wuyts, M. Babanezhad, T. Wuytack, S. Adriaenssens and R. Samson, Tree Leaf Wettability as Passive Bio-Indicator of Urban Habitat Quality, *Environ. Exp. Bot.*, 2012, **75**, 277–285.
54 C. Larue, H. Castillo-Michel, S. Sobanska, N. Trcera, S. Sorieul, L. Cécillon, L. Ouerdane, S. Legros and G. Sarret, Fate of Pristine TiO2 Nanoparticles and Aged Paint-Containing TiO2 Nanoparticles in Lettuce Crop after Foliar Exposure, *J. Hazard. Mater.*, 2014, **273**, 17–26.
55 J. Kurepa, T. Paunesku, S. Vogt, H. Arora, B. M. Rabatic, J. Lu, M. B. Wanzer, G. E. Woloschak and J. A. Smalle, Uptake and Distribution of Ultrasmall Anatase TiO_2 Alizarin Red S Nanoconjugates in Arabidopsis Thaliana, *Nano Lett.*, 2010, **10**(7), 2296–2302.
56 J. Hong, C. M. Rico, L. Zhao, A. S. Adeleye, A. A. Keller, J. R. Peralta-Videa and J. L. Gardea-Torresdey, Toxic Effects of Copper-Based Nanoparticles or Compounds to Lettuce (Lactuca Sativa) and Alfalfa (Medicago Sativa), *Environ. Sci.: Processes Impacts*, 2014, **17**(1), 177–185.
57 C. Larue, J. Laurette, N. Herlin-Boime, H. Khodja, B. Fayard, A.-M. Flank, F. Brisset and M. Carriere, Accumulation, Translocation and Impact of TiO2 Nanoparticles in Wheat (Triticum Aestivum Spp.): Influence of Diameter and Crystal Phase, *Sci. Total Environ.*, 2012, **431**, 197–208.
58 D. Lin and B. Xing, Root Uptake and Phytotoxicity of ZnO Nanoparticles, *Environ. Sci. Technol.*, 2008, **42**(15), 5580–5585.
59 K. Birbaum, R. Brogioli, M. Schellenberg, E. Martinoia, W. J. Stark, D. Günther and L. K. Limbach, No Evidence for Cerium Dioxide Nanoparticle Translocation in Maize Plants, *Environ. Sci. Technol.*, 2010, **44**(22), 8718–8723.
60 A. Valletta, L. Chronopoulou, C. Palocci, B. Baldan, L. Donati and G. Pasqua, Poly(Lactic-Co-Glycolic) Acid Nanoparticles Uptake by Vitis Vinifera and Grapevine-Pathogenic Fungi, *J. Nanopart. Res.*, 2014, **16**(12), 2744.
61 M. Uyttendaele, L. Jacxsens and S. Van Boxstael, 4 - Issues Surrounding the European Fresh Produce Trade: A Global Perspective, in *Global Safety of Fresh Produce*, ed. J. Hoorfar, Woodhead Publishing, 2014, pp. 33–51.
62 Y. Song, B. A. Maher, F. Li, X. Wang, X. Sun and H. Zhang, Particulate Matter Deposited on Leaf of Five Evergreen Species in Beijing, China: Source Identification and Size Distribution, *Atmos. Environ.*, 2015, **105**, 53–60.

